LA-UR-91-2283

LA-UR--91-2283

DE91 016041

TITLE DIAGNOSIS OF NONLINEAR SYSTEMS USING TIME SERIES ANALYSIS

AUTHOR(S) N. F. Hunter, NX-11

SUBMITTED TO 3rd Int'l Machinery Monitoring Conf.
Las Vegas, NV
Dec. 9-12, 1991

DISCLAIMER

Los Alamos National Laboratory
Los Alamos, New Mexico 87545

DIAGNOSIS OF NONLINEAR SYSTEMS USING TIME SERIES ANALYSIS

by
Norman F. Hunter, Jr.
Dynamic Testing Section
Group WX-11
Los Alamos National Laboratory

ACKNOWLEDGEMENTS

Grateful acknowledgement is made for the assistance of a number of individuals, including J. Doyne Farmer, Stephen Eubank, and John Gibson, Group T-13, Los Alamos National Laboratory, Martin Casdagli of the Santa Fe Institute, and Wallace Larimore of Adaptics, Inc.

ABSTRACT

Diagnosis and analysis techniques for linear systems have been developed and refined to a high degree of precision. In contrast, techniques for the analysis of data from nonlinear systems are in the early stages of development. This paper describes a time series technique for the analysis of data from nonlinear systems. The input and response time series resulting from excitation of the nonlinear system are embedded in a state space. The form of the embedding is optimized using local canonical variate analysis and singular value decomposition techniques. From the state space model, future system responses are estimated. The expected degree of predictability of the system is investigated using the state transition matrix. The degree of nonlinearity present is quantified using the geometry of the transfer function poles in the z plane. Examples of application to a linear single-degree-of-freedom system, a single-degree-of-freedom Duffing Oscillator, and linear and nonlinear three degree of freedom oscillators are presented.

NOMENCLATURE

f	response frequency.
x(t)	sampled input time series to an experimental system. (may be univariate or multivariate).
y(t)	sampled response time series from an experimental system. (may be univariate or multivariate).

τ	sample interval for digitally sampled data.
j	number of lags used in embedding the response time series.
l	number of lags used in embedding the input time series.
a_i	coefficients of the ith delayed input term in a linear time series model.
b_i	ccefficients of the ith delayed response term in a linear time series model.
ω_n	angular natural frequency foz a linear oscillator.
ζ	damping ratio for a linear oscillator.
α	coefficient of the anti-symmetric quadratic term for base excited nonlinear oscillator.
β	coefficient of the symmetric quadratic term for base excited nonlinear oscillator.
y_c"	input acceleration to the base of the single degree of freedom oscillator.
y"	response acceleration for the single degree of freeaom base excited oscillator.

INTRODUCTION

Consider the system described in Figure 1. This unknown system is excited by an input time series u(t), which in the context of mechanical vibrating systems, is typically a measured force or acceleration, and responds with a response time series y(t), typically acceleration or strain. The input and response time series, shown here as univariate, may in general be multivariate, consisting of multiple inputs and responses.

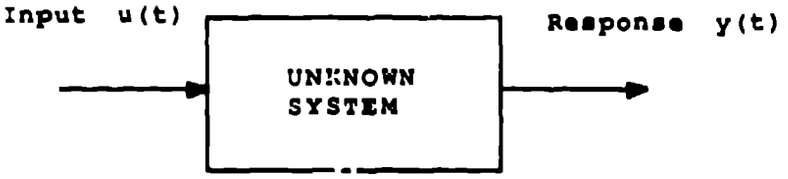

Figure 1
Conceptual Input-Output System
In this figure the system is viewed as a "black box", defined by its response y(t) to an input time series u(t).

If the system is linear, the analysis techniques typically use the Fourier transformation to obtain input and response data in the frequency domain. Frequency domain data is then used to provide response power spectra and transfer function estimation. Peaks in the transfer function indicate resonant frequencies, or modes, of the linear system, and provide considerable insight into the system dynamics. Fourier techniques are

very effective for the analysis of linear systems as they provide a relatively simple means of characterizing a system from experimentally derived test data.

For a nonlinear system, the use of Fourier transformation techniques, coupled with random excitation, produces the best fit linear estimate of the systems behavior.

Fitting a linear model to a dynamic system is appropriate if the system's behavior is nearly linear. For strongly nonlinear systems, however, the transfer function does a poor job of modelling the real system, either in terms of the effective number of degrees of freedom or in terms of prediction of the system's behavior. In fact, nonlinear systems behave in a manner fundamentally different and more complex than do linear systems. The principle of superposition holds for linear systems, making it easy to separate transient and steady state system responses. For nonlinear systems, however, superposition does not hold, so the simplification of a response into transient and steady state components cannot be made in the same manner. Further, nonlinear systems are frequency creative. A linear system excited by a frequency f_0 responds at the same frequency f_0. In contrast, nonlinear systems readily transfer energy between frequencies. An example of this energy transfer is shown in Figure 2, where two examples of the response waveforms produced by a strongly nonlinear, mechanical oscillator (two well potential systems) driven by a sine wave are illustrated.

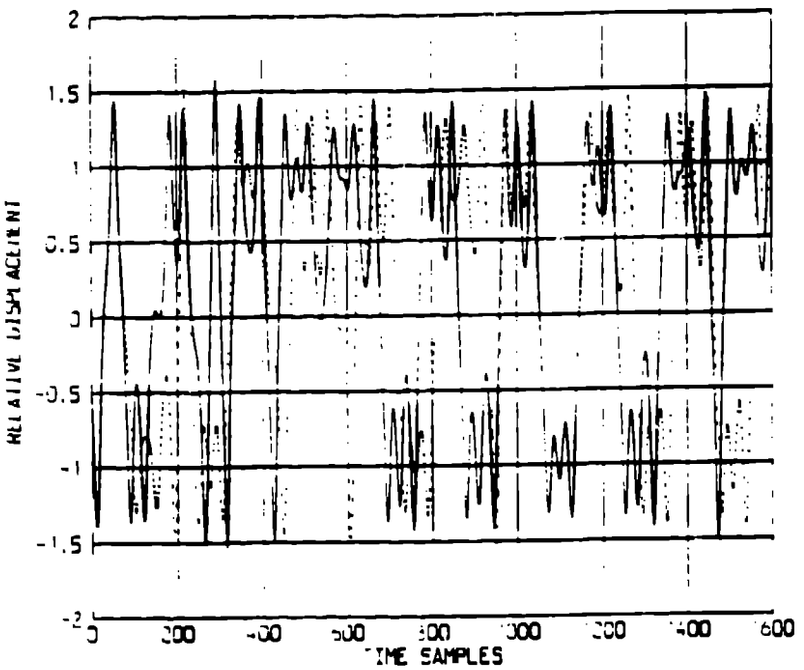

Figure 2
Response of a Single Degree of Freedom Two-Well-Potential System

Even though, in two separate cases, the system is excited by a sine wave, the response waveforms illustrated by the solid and dotted lines are not periodic. In fact this is an example of chaotic behavior.

Note that the response of this system is not even periodic. The concept of chaotic behavior has recently been applied to nonlinear systems. In a chaotic system, a high degree of sensitivity to the initial conditions exists, so that infinitesimal changes in the system state lead, in finite time, to different time series behaviors. Many strongly nonlinear systems are chaotic, even when excited by sinusoidal inputs[1]. Figure 3 illustrates the effect of a one percent perturbation in the state of a chaotic, sinusoidally excited, duffing oscillator. The perturbed and unperturbed responses diverge with time, producing two different time series responses. The concept of chaotic behavior as sensitivity to initial conditions also occurs in systems driven by random inputs.

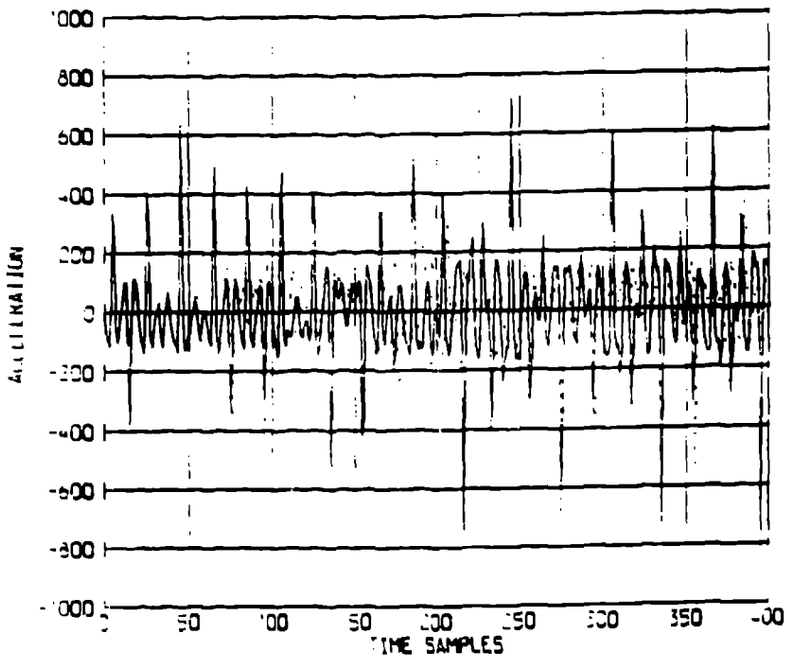

Figure 3
Deviation of Responses For A 1% Difference in States for A Strongly Nonlinear Duffing Oscillator.
Note the gradual deviation between the solid and dashed waveforms until two completely uncorrelated time responses occur.

There are several ways to approach the problem of characterizing a nonlinear system from test data. The frequency response function approach may be extended to nonlinear systems through the use of Volterra or Weiner Series[3]. These approaches extend the transfer function concept to higher order spectra, where the response at a frequency f_1 is produced by a set of frequencies which sum to f_1.

In our approach we analyze nonlinear systems by fitting the input and response time series to derive a set of "locally linear", but globally nonlinear, models of the system behavior. This formulation allows us to predict the long term response of the system (for nonchaotic systems) and the short term response for systems which are chaotic. Nonlinearity is detected by observing changes in the local behavior as we successively model the time series response in different parts of the state space.

MODEL FORMULATION.

Consider the system which is illustrated in Figure 1. The input and response time series are sampled with sample interval τ. The response time series forms an image of the state of the system. This image may be reconstructed using delay coordinates in place of the unobserved state variables[4]. In a delay coordinate formulation the future response of the system is a function of the past responses and current and delayed inputs as shown in Equation 1:

$$y(t) = f\{ y(t-\tau), y(t-2\tau), \ldots y(t-j\tau), u(t), u(t-\tau), u(t-2\tau), \ldots u(t-l\tau)\} \quad (1)$$

For a linear system this formulation is a linear one and we write:

$$y(t) = b_1 y(t-\tau) + b_2 y(t-2\tau) + \ldots + b_j u(t-j\tau) + a_1 + a_1 u(t-\tau) + a_2 u(t-2\tau) + \ldots + a_l u(t-l\tau) \quad (2)$$

The formulation of Equation 2 is, of course, the well known ARMA, or autoregressive moving average model which is often used in the time series modelling of linear systems. A fundamental problem in applying the ARMA technique to a nonlinear system is in the determination of the proper functional form to use in Equation 1. Some natural choices of functional forms include polynomials, radial basis functions, and splines[5,6,7]. The problem of fitting a function to Equation 1 is essentially one of surface fitting, as illustrated in Figure 4, where, for purposes of illustration, the current $y(t)$ is depicted as a function of the two variables $u(t)$ and $y(t-\tau)$.

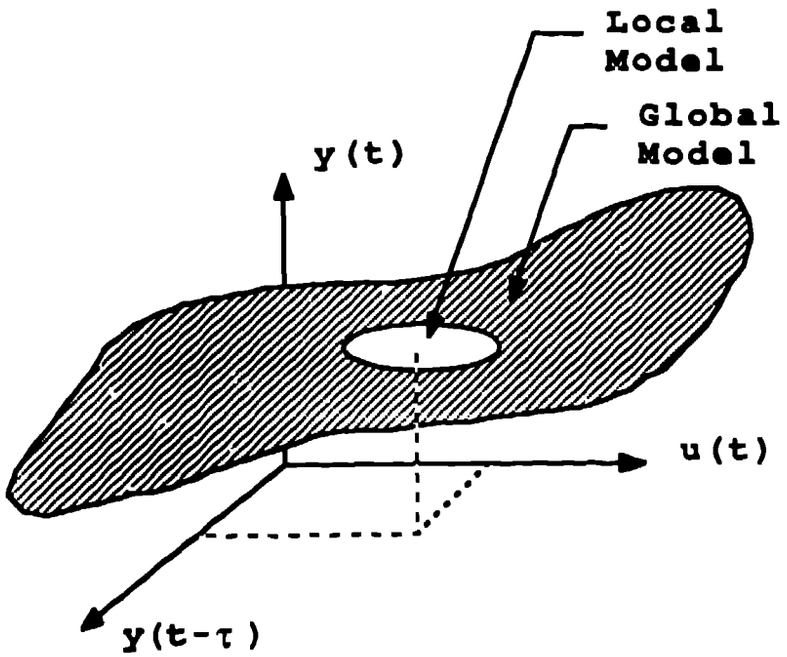

Figure 4
A Simplified Illustration of the Solution of Equation 1 as a Problem in Surface Fitting.
Here the current y(t) is depicted as a function of the input, u(t), and the past response, y(t-τ). The surface fitting may be accomplished globally as shown by the shaded entire surface, or locally, as shown by the clear elliptical region.

One efficient means of fitting the surface of Figure 4 is through the use of local techniques. Only points in the neighborhood of the past values for which prediction is desired are used to solve the model. Many functional forms may be used for local surface fitting, including the linear form of Equation 2, as long as the function is reapplied in each region for which prediction is desired. We have used global polynomials, global radial basis functions, and local linear models in attempting to model nonlinear systems. Of these forms, the best results were obtained using local linear models.

Embedding Techniques

Our image of the state space in equations 1 and 2 is formed in a space where each coordinate is one of the delayed u(t) or y(t) terms. The dimension of the space is effectively n+1, or the number of input terms plus the number of response terms, possibly plus a constant term. This may be a very inefficient representation of the system state, with a dimension larger than is required. Too large a dimension implies inefficient fitting of

the function which relates the past to the future. Two approaches have been taken to alleviate this dimensionality problem, Singular Value Decomposition[9] and Canonical Variate Analysis[10]. We have used both of these approaches, and both essentially provide an estimate of the number of effective states in the systems by using coordinates which are formed from a linear combination of the delay coordinates. The singular value decomposition technique is applied primarily to autonomous systems (systems modelled using only the response signal), and the canonical variate analysis technique to driven systems. To date, the most effective approach we have found for driven systems uses the local canonical variate analysis technique, the details of which are described in the references[11].

Iterative Prediction

The prediction of a given value y(t) from past values of y(t) and u(t) is useful but for many purposes incomplete, as we often desire to predict future response waveforms consisting of many individual sample intervals. To achieve this form of prediction we iteratively predict the response, using successive y(t)'s as past values of the response as they are computed Equations 3 illustrate the iterative prediction process.

$$y(t_0) = f\{ y(t_0-\tau), y(t_0-2\tau), \ldots y(t_0-j\tau), u(t_0), u(t_0-\tau), u(t_0-2\tau), \ldots u(t_0-1\tau)\} \quad (3a)$$

$$y(t+\tau) = f\{ y(t_0), y(t_0-\tau), \ldots y(t_0-(j-1)\tau), u(t_0+\tau), u(t_0), u(t_0-\tau), \ldots u(t_0-(1-1)\tau)\} \quad (3b)$$

First our model is applied to solve for $y(t_0)$ as shown in Equation 3a. The $y(t_0)$ computed from (3a) then serves an an input to a succeeding model in (3b), where the computed value of $y(t_0+\tau)$ serves as the input to a second iteration which solves for $y(t_0+2\tau)$. These "iterative" predictions are repeated many times for succesively increasing τ values to obtain the estimated response waveshape over long time periods. All of the predictions shown in this paper are iterated predictions over the time range indicated in the figures. An iterated prediction is a demanding test of a model since it requires consistently accurate predictions. Of course, a direct comparison of the response and the iterated prediction may show that the predicted and measured waveforms diverge if the system behaves chaotically, so another measure of model validity, such as the power spectrum, must be used in instances of chaotic behavior.

A summary of the complete algorithm for characterization and response prediction for nonlinear systems is shown in Figure 5.

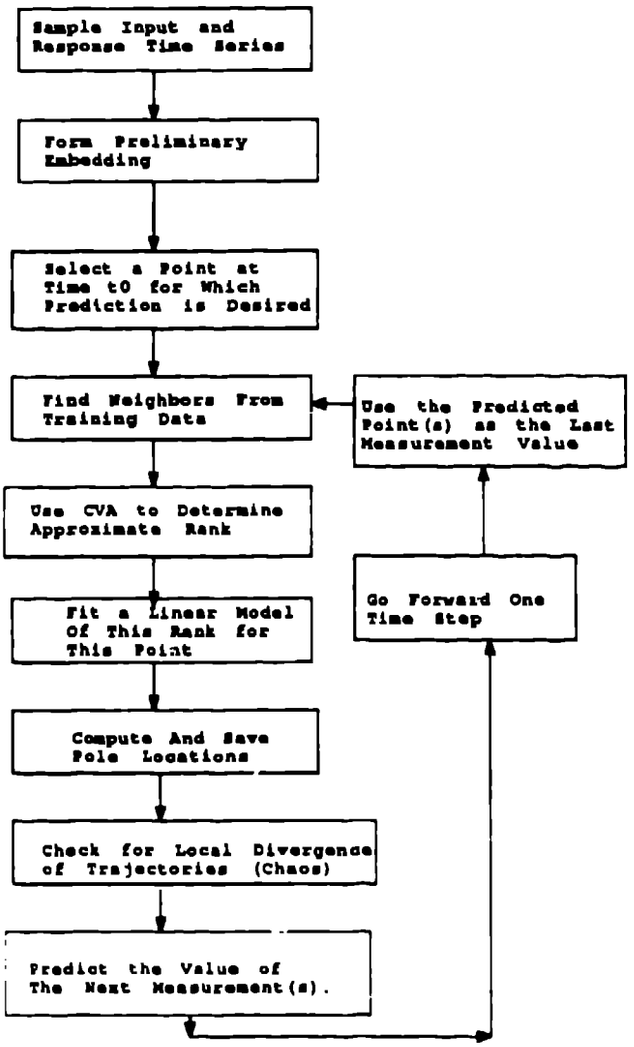

Figure 5
Algorithm for Response Prediction and Characterization of a Nonlinear System
This algorithm uses the input time series, assumed known at all times, and the response time series, which is known only during a training period.

We have implemented the algorithm in Matlab (a higher level matrix analysis language) and also, in some forms, in C. The steps in this algorithm are followed sequentially for all of the examples used in this paper.

System Characterization

The steps shown in Figure 5 define an algorithm for the prediction of responses of nonlinear systems using a local linear model. Since our model is "locally" linear, at each time t_j we have an estimate of the transfer function in the form of Equation 4.

$$h_t = (a_0 + a_1 z^{-1} + a_2 z^{-2} + \ldots + a_j z^{-j}) / (b_0 + b_1 z^{-1} + b_2 z^{-2} + \ldots b_1 z^{-1}) \quad (4)$$

As we sweep through the time series response for the system, successively computing estimates of the current response, we have, at each time t, an estimate of the transfer function. If the system is linear, this estimate is consistent at every time step. For a nonlinear system, in contrast, the effective transfer function varies with the time(fundamentally with the differing states) at which the transfer function is computed. We chose to characterize the transfer function by the location of the transfer function poles in the z plane. We will observe the location of these poles in several linear and nonlinear systems.

EXAMPLES.

Single Degree of Freedom Linear Oscillator

A single degree of freedom linear, force excited, oscillator is shown in Figure 6. The oscillator has a resonant frequency of f_n=1 Hz. and ζ=2% damping.

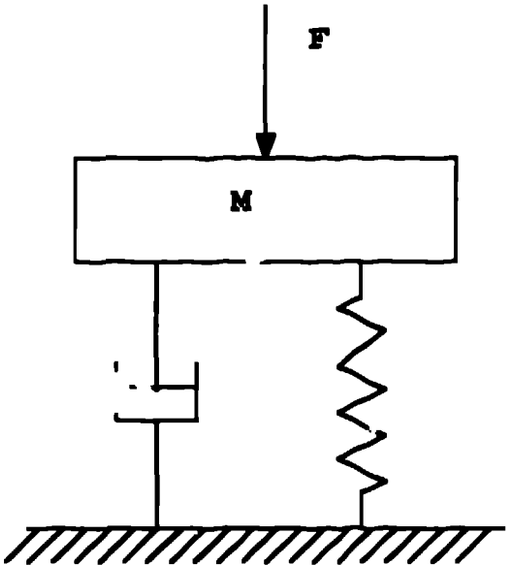

Figure 6a
Linear, Force Excited Single Degree of Freedom Oscillator.

The oscillator is excited by band limited random noise and 2000 samples of the input and response waveforms used as training data for system characterization. Eight input and eight response lags are used in the embedding and local CVA applied. The number of significant singular values indicates that a state rank of three is appropriate. The local linear CVA model is then applied to predict 200 samples into the future as shown in Figure 6b.

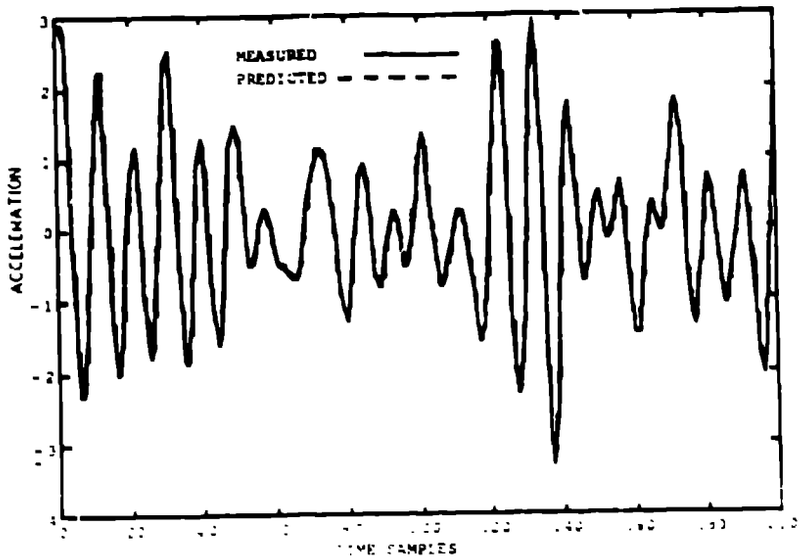

Figure 6b.
Measured and Predicted Responses for the Single Degree of Freedom Linear Oscillator Excited by Band Limited Random Noise.
The measured waveform (solid) and predicted waveform(dashed) can scarcely be distinguished.

Accurate iterated predictions are obtained for the entire sample interval, indicating that our model is valid. As each sample is predicted we can observe the pole locations of the transfer function in the z plane. These pole locations are shown in Figure 6c.

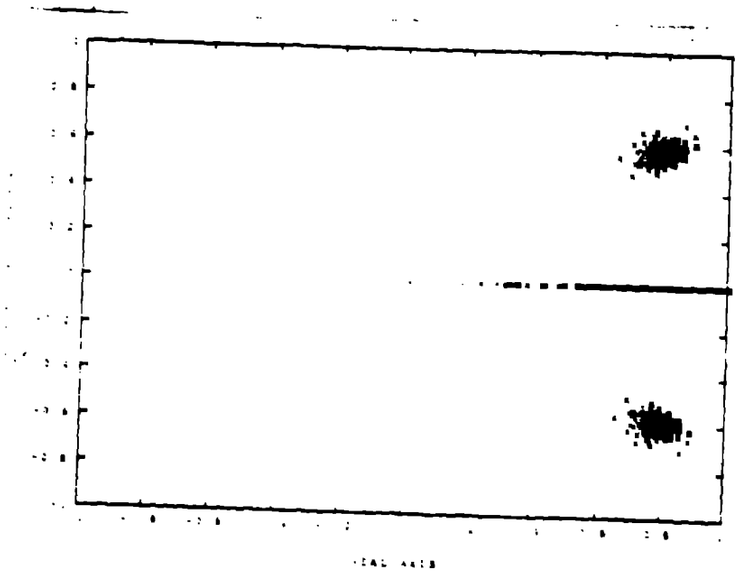

Figure 6c
Pole Locations for the Linear Oscillator.
Note the tight clustering of the poles in two discrete, conjugate locations, indicating that a single resonant frequency is present, as expected.

The tight clustering of the two poles shown in Figure 6c indicates that the system has a single, consistent, resonant frequency. The implication is, as expected, that we are observing data from a linear system.

Nonlinear Duffing Oscillator

We now simulate the Duffing-like oscillator of Equation 5 and Figure 7, using an analog computer.

$$y'' + 2\zeta\omega_n(y'-y_0') + \omega_n^2(y-y_0) + \alpha(y-y_0)^2 + \beta(y-y_0)|y-y_0| = 0 \qquad (5)$$

Note: Typically the Duffing oscillator contains a cubic stiffness term. Here, for ease of simulation, asymmetric and anti-asymmetric quadratic terms are used.

ω_n = $2\pi(10.2)$
ζ = .24
α = 1.00
β = 1.00
y'' = acceleration of the base of the system.
y_1'' = response acceleration.

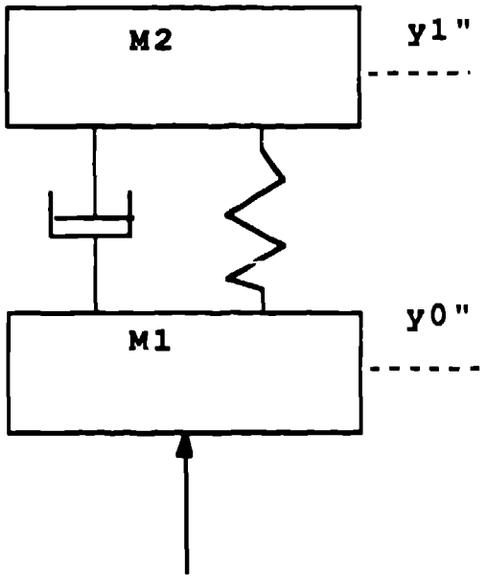

Figure 7
Base Excited Nonlinear Duffing-Like Oscillator

In contrast to the linear oscillator this system is excited using a base acceleration.

The oscillator is excited using a Genrad 2514 random vibration controller and input and response signals digitized using a Masscomp 5520 computer system. 2000 points of the input and response signals are used in the training data set and local linear CVA applied. A state rank of three is indicated by the number of significant singular values. The model is used to predict the time response for a period of 200 samples. Measured response and iterated prediction are shown in Figure 8a.

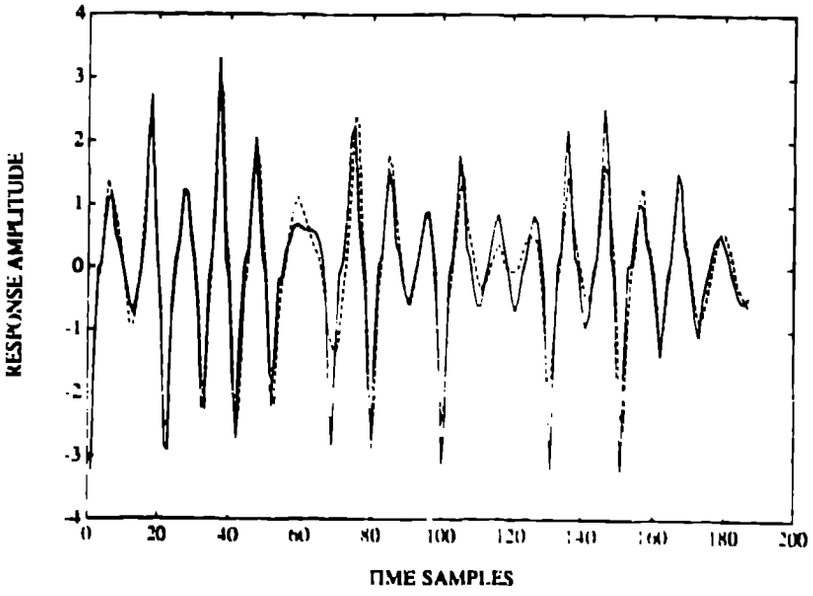

Figure 8a.
Measured and Iterated Predictions for the Response of the Duffing Oscillator.
The measured response (solid curve) and the Iterated prediction (Dashed curve) compare favorably for this form of nonlinear model, even for an iterated prediction.

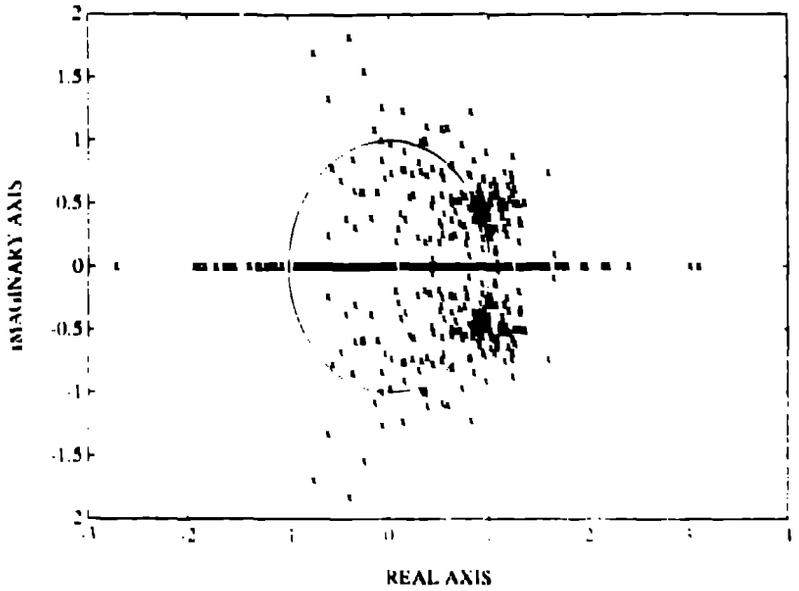

Figure 8b.
Pole Locations Observed for the Duffing-Like Oscillator.

Unlike the linear system, the pole locations are diffuse, indicating that the system's effective resonant frequency shift with time, or more accurately, with the instantaneous state of the system. Note the that the model is locally unstable, as indicated by poles locally outside the unit circle.

The model, while not quite as accurate as the model for the linear system, does a respectable job of predicting the response of this strongly nonlinear oscillator over the range of samples illustrated. We do not show the results of a linear model, which failed to predict even the general waveshape of the response illustrated here. Pole locations for this system are shown in Figure 8b. Unlike the linear system, the pole locations vary with where we are in the time series, indicating the presence of significant nonlinearity.

Three Degree of Freedom Oscillator

To illustrate the application of this type of model to a multi degree-of-freedom system, we chose the system illustrated in Figure 9a. Here a four mass, three spring system is excited with band limited random noise. We consider two cases; Case I: all stiffnesses and dampings linear and equal. Case II: All parameters identical to Case I except the stiffness connecting masses 1 and 2 is nonlinear with stiffness 10 greater when the

relative displacement between masses 2 and 3 is negative. Initially $k10=k12=k13=2\pi(1.0)$ and all damping coefficients
$c10=c12=c13=2\zeta wn = 2(.02)2\pi(1.0)$.

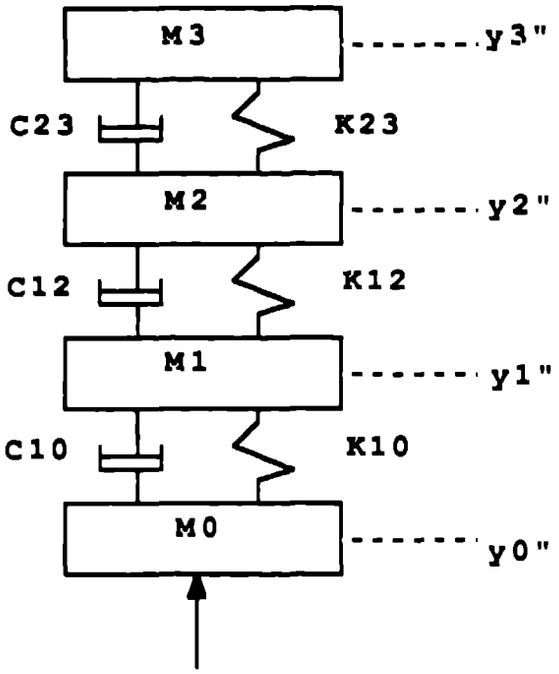

CASE I: K12 LINEAR
CASE II: K12 BILINEAR

Figure 9a.
Diagram of a Three Degree of Freedom Oscillator.

Note that the oscillator may be linear (K12 linear) or nonlinear (K12 bilinear) as indicated. The input signal is the base acceleration y_0". Responses are the accelerations y_3", y_2", and y_1".

In each case we apply the local linear CVA model to 4000 training data points from the system, which consists of the input time series and the response accelerations of masses 1,2, and 3. As in the case for the linear single-degree-of-freedom oscillator, measured and predicted responses virtually overlay. The pole locations for the linear system lie in 6 distinct conjugate regions, as shown in Figure 9b. There are three pairs of complex conjugate pole locations, indicating the presence of three distinct, associated resonant frequencies. These pole locations are as expected from an analytical analysis of the differential equations governing the system. The eigenvalues of the system state transition matrix indicate the overall degree of predictability for the state transitions. In Figure 9c these eigenvalues are

plotted for the range of sample points considered. The eigenvalues remain less than unity over the entire range, indicating that the system is predictable.

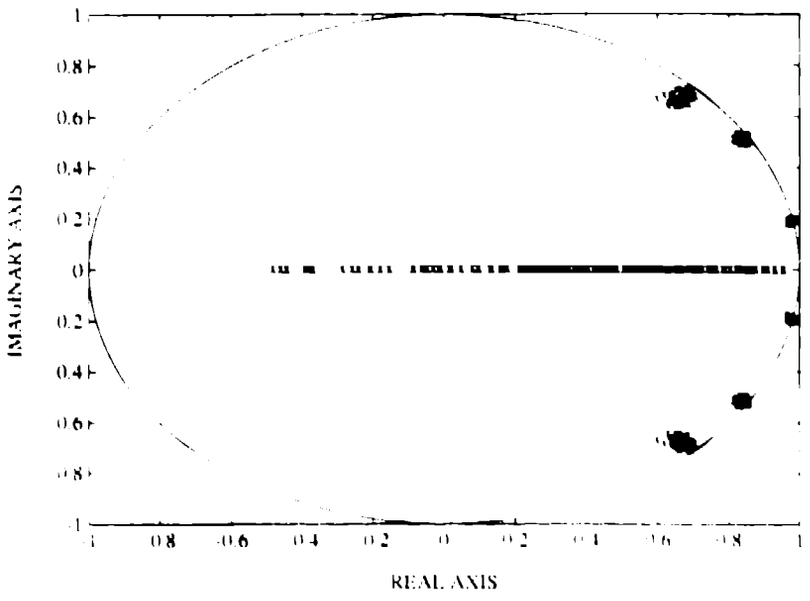

Figure 9b.
Pole Locations, as Indicated From Measured Response Data, for the Three Degree of Freedom Linear Oscillator.
Note that three consistent resonant frequencies exist at locations which an analysis of the system predicts.

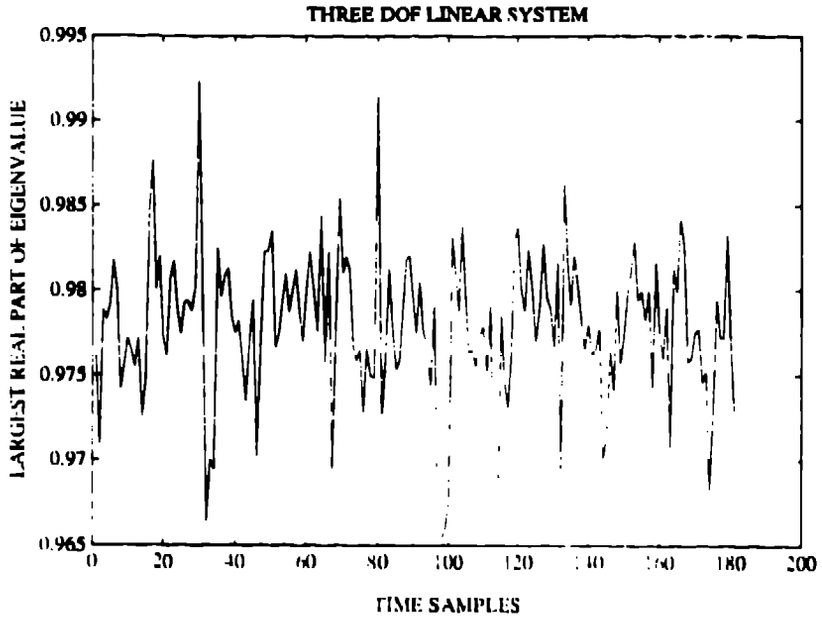

Figure 9c
Real Part of the Largest Eigenvalue for The Linear 3 DOF State Transition Matrix
Note that the largest eigenvalue does not exceed unity.

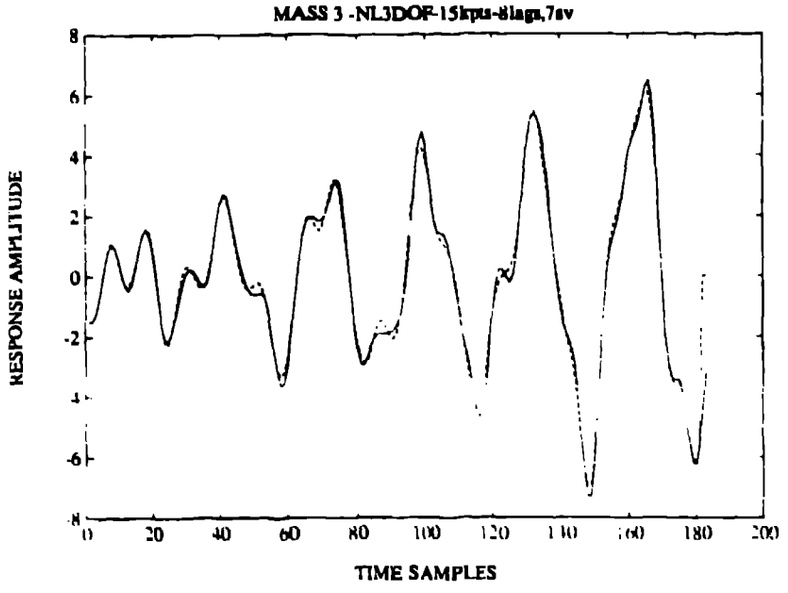

Figure 9d.
Measured and Predicted Time Series for a Segment of The Response of Mass 3 for the Nonlinear Case of Figure 9a.
Note the relatively good comparison between the measured (solid line) and predicted (dashed line) responses over this time span.

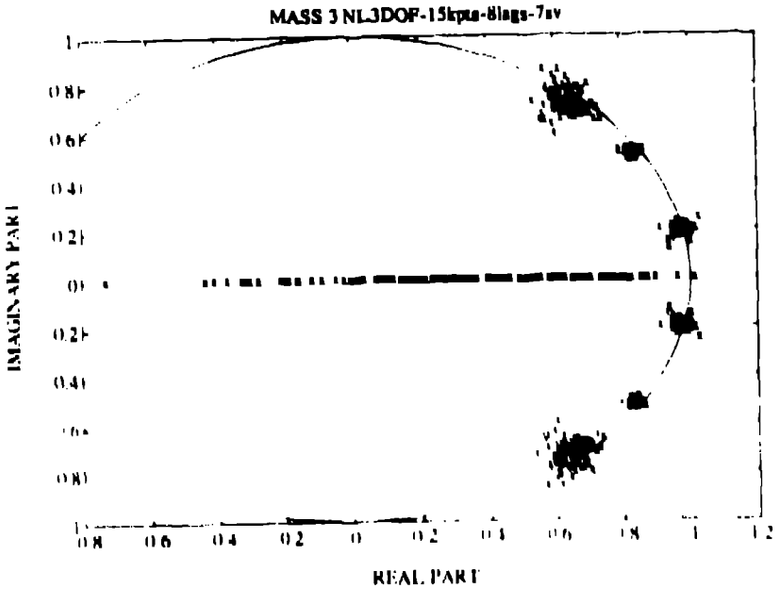

Figure 9e.
Pole Locations for the Nonlinear Oscillator as Indicated by the Local Linear CVA Model.
Two pole locations are relatively insensitive to the nonlinearity. The third pole location is

smeared into an elliptical range by the presence of the nonlinear stiffness k_{12}.

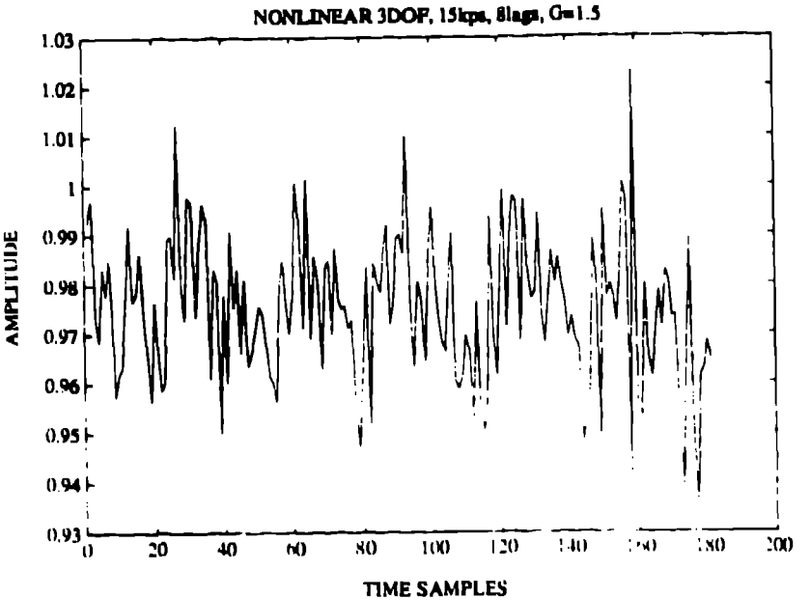

Figure 9f
Real Part of the Largest Eigenvalue for The Nonlinear 3 DOF State Transition Matrix
Note that the largest eigenvalue now exceeds unity locally in several regions.

We now consider the nonlinear case, illustrated in figures 9d 9e, and 9f. We apply local linear CVA to 10,000 training data points. Measured and predicted acceleration responses of mass 3 are compared in Figure 9d for 200 data points outside the training interval. The comparison, while not as good as that obtained for a linear system, is judged sufficiently accurate to indicate that the model is valid. Pole locations for this three degree of freedom nonlinear oscillator are shown in Figure 9e. In comparison to the linear oscillator, two sets of pole locations remain fairly consistent, but the location of the third pole has changed into two poles located near the imaginary axis. This system appears to have four conjugate pole locations but the state rank of the system is seven, just as in the linear case. Consequently we are observing the effects of a nonlinearity. The double pole location is consistent with two stiffnesses in location k_{12}. The shift in the location of the double pole indicates that this effective resonant frequency of the system varies with the system state, indicating the presence of significantly nonlinear behavior. Analysis of the system indicates that the double pole is more sensitive to variations in

k_{12} than are the other poles, whose locations change only minimally.

CONCLUSION

We have illustrated a method for the analysis of nonlinear systems which makes use of a segment of the input and response waveforms for the system (training data) to build a system model. This model provides, through geometry of the pole locations in the z plane, an estimate of the degree of nonlinearity of the system. Future time series responses of the system under study are predicted. Further application of this model formulation to a greater variety of nonlinear systems is planned. Some features of the model include:

1. Training data used must explore the same regions of the state space as those for which response prediction is desired. Extrapolation to unexplored regions of the state space is limited.

2. Training point requirements will probably range between thousands and hundreds of thousands of points, depending on system complexity.

3. Multiple response measurements are desirable when analyzing complex systems.

4. The number of significant singular values gives an estimate of the state rank of the system.

5. Running time for the algorithm is on the order of 20 minutes for the systems illustrated using a Sun Sparkstation. There are potential gains in algorithmic efficiency which have not yet been utilized.

6. The algorithm gives an indications of regions of the time series where prediction may be difficult.

7. Information theoretic criteria relating to the model require further investigation and clarification, especially in determining the best means of embedding and in determining the number of data points required for training.

At this point the technique looks promising for the detection of nonlinearity in dynamic systems and for the prediction of the time series response (for non-chaotic regions) or the response statistics (for chaotic regions). The use of this technique is not limited to data from mechanical oscillators but may be applied to a wide variety of systems of low to moderate state rank where input and response time series are available.

REFERENCES

1.Moon, Chaotic Vibrations, Wiley, 1987.

2. Casdagli, Martin, A Dynamical System Approach to Driven Systems, Proceedings of the Nato Conference on Dynamic Systems, Santa Fe Institute, Santa Fe, New Mexico, October, 1990.

3.Powers, E.J., Hong, J. Y., and Kim, Y.C., "On Modelling the Nonlinear Relationship Between Fluctuations with Nonlinear Transfer Functions", Proceedings of the IEEE, Vol. 68, No. 8, Aug. 1980.

4. Farmer, J. Doyne, and Sidorowich, John J. , "Exploiting Chaos to Predict the Future and Reduce Noise", Los Alamos National Laboratory Technical Report 88-901., March 1988.

5. Billings, S. A., Tsang, K. M., and Tomlinson, G. R., "Application of the Narmax Method to Nonlinear Frequency Response Estimation, Proceedings of the 6th International IMAC Conference, 1987, p. 1433-1438.

6. Casdagli, Martin, "Nonlinear Prediction of Chaotic Time Series", Physica D, May 1988.

7.Friedman, Jerome H., "Multivariate Adaptive Regression Splines", Technical Report No. 102, Department of Statistics, Stanford, University, 1989.

8.Casdagli, Martin,Gibson, John,Eubank, Stephen, Farmer, J. Doyne, State Space Reconstruction in the Presence of Noise, Submitted to Physica D, October, 1990 .

10.Larimore, W.E., "System Identification, Reduced Order Filtering, and Modelling Via Canonical Variate Analysis, Proceedings of 1983 American [illegible] Conference.

11. Hunter, Norman F., Application of Time Series Models to Nonlinear Systems, Proceedings of the 47 Annual IES Conference, 1991.